Voltammetry of a Flavocytochrome c_3: The Lowest Potential Heme Modulates Fumarate Reduction Rates

Julea N. Butt,* Jeremy Thornton,† David J. Richardson,† and Paul S. Dobbin†
Schools of *Chemical and †Biological Sciences, Centre for Metalloprotein Spectroscopy and Biology, University of East Anglia, Norwich NR4 7TJ, United Kingdom

ABSTRACT Iron-induced flavocytochrome c_3, Ifc_3, from *Shewanella frigidimarina* NCIMB400, derivatized with a 2-pyridyl disulfide label, self-assembles on gold electrodes as a functional array whose fumarate reductase activity as viewed by direct electrochemistry is indistinguishable from that of Ifc_3 adsorbed on gold or graphite electrodes. The enhanced stability of the labeled protein's array permits analysis at a rotating electrode and limiting catalytic currents fit well to a Michaelis-Menten description of enzyme kinetics with $K_M = 56 \pm 20$ μM, pH 7.5, comparable to that obtained in solution assays. At fumarate concentrations above 145 μM cyclic voltammetry shows the catalytic response to contain two features. The position and width of the lower potential component centered on -290 mV and corresponding to a one-electron wave implicates the oxidation state of the lowest potential heme of Ifc_3 as a defining feature in the mechanism of fumarate reduction at high turnover rates. We propose the operation of dual pathways for electron transfer to the active site of Ifc_3 with the lowest potential heme acting as an electron relay on one of these pathways.

INTRODUCTION

In addition to their catalytic centers, redox enzymes often contain multiple redox cofactors that may serve either to provide electron transfer routes through the protein matrix or to modulate enzyme activity through an oxidation state change. Together the cofactors act as an ensemble, coupling electrochemical and chemical events to define the enzyme's catalytic behavior. Such systems can achieve considerable complexity, as illustrated by two components of the mitochondrial respiratory chain (Saraste, 1999); in heme-copper oxidases coordinated electron and proton transfer during the reduction of oxygen to water results in proton translocation, while a bifurcated electron transfer pathway in the cytochrome bc_1 complex drives the Q-cycle in parallel with cytochrome *c* reduction.

A large number of redox enzymes directly couple two-electron transformation of substrate to one-electron redox cofactors such as hemes or iron-sulfur clusters (Chapman et al., 1999). The iron-induced tetraheme flavocytochrome c_3 (Ifc_3) from *Shewanella frigidimarina* NCIMB400 is an example of one such protein (Dobbin et al., 1999). This soluble, 63.9 kDa, multicentered redox protein possesses unidirectional fumarate reductase activity, and folds in three domains (Bamford et al., 1999b, Dobbin et al. 1999). The active site, a noncovalently bound, low potential flavin adenine dinucleotide (FAD) is coordinated by one of the C-terminal domains, while four *c*-hemes, midpoint potentials -73, -141, -174, and -259 mV (pH 7.5) are bound by the smaller N-terminal domain. The hemes of Ifc_3 may play a role in electron delivery to the active site; intramolecular heme-flavin electron transfer has been implicated as a decisive factor in the mechanisms of lactate dehydrogenation by *Saccharomyces cerevisiae* flavocytochrome b_2 (Daff et al., 1996) and fumarate reduction by *S. frigidimarina* flavocytochrome c_3 (Fcc_3) (Turner et al., 1999).

Direct protein electrochemistry is emerging as a powerful method with which to probe biological electron transfer. Most obviously the reduction potentials of redox cofactors can be determined (Armstrong, 1990). However, by providing a description of the redox protein's activity in real time over a wide and continuous potential window, such experiments also provide a kinetic description of electron transfer which is most readily defined in the diffusionless electrochemical response of proteins immobilized as (sub)monolayers on the electrode surface (Armstrong et al., 1997). When the rate of electron exchange between electrode and electroactive protein film is sufficiently fast as to be non-rate-limiting, the kinetic parameters describing chemical transformations of redox cofactors can be determined (Hirst et al., 1998a, b; Butt et al., 1993). Most recently, the ability of direct electrochemical methods to reveal subtleties in the intramolecular electron transfer dynamics of multicentered redox enzymes has been highlighted (Heering et al., 1997, 1998; Armstrong et al., 1997; Hirst et al., 1996). Protein film voltammetry of two fumarate reductases, the iron-sulfur cluster and flavin-containing FrdAB subunits of the membrane anchored *Escherichia coli* enzyme (Heering et al., 1997) and the soluble tetraheme- and flavin-containing Fcc_3 from *S. frigidimarina* (Turner et al., 1999), has demonstrated that intramolecular electron transfer from their respective one electron redox cofactors contributes significantly to the definition of each enzyme's catalytic operation.

We have previously reported cyclic voltammetry of Ifc_3 solutions in which complex waveforms composed of overlapping contributions from the FAD and heme centers are observed (Dobbin et al., 1999). On addition of fumarate the

Received for publication 16 June 1999 and in final form 4 October 1999.
Address reprint requests to Julea N. Butt, School of Chemical Sciences, University of East Anglia, Norwich NR4 7TJ, UK. Tel.: 44-1603-593877; Fax: 44-1603-592003; E-mail: j.butt@uea.ac.uk.

0006-3495/00/02/1001/09 $2.00

waves are transformed into the sigmoidal form typical for reductive electrocatalysis. However, direct electrochemical studies of the intrinsic properties of Ifc_3 would be facilitated by immobilizing the enzyme on an electrode surface and performing voltammetry under conditions that reflect rate-limiting events intrinsic to the enzyme. To ensure that substrate depletion at the electrode surface does not influence the electrocatalytic response, experiments should be performed under conditions where the supply of substrate to the enzyme exceeds the rate of turnover. This may be achieved by employing radial diffusion of substrate to a microelectrode (Wightman, 1981), although most reports to date exploit spontaneous adsorption of protein films to a macroelectrode that is rapidly rotated to drive substrate to the electrode surface by forced convection (Bard and Faulkner, 1980). Unfortunately, adsorbed Ifc_3 films were unstable on electrode rotation, which prevented detailed analysis of the system of interest. Therefore, we have sought a method for covalent attachment of Ifc_3 to an electrode surface that may be generally applicable to the study of redox proteins by film voltammetry.

The adsorption of organothiols on gold accompanied by covalent gold-sulfur bond formation results in stable two-dimensional arrays ideally suited for electrochemical studies (Weber and Creager, 1994; Chidsey, 1991). Such methods have been extensively exploited in the development of mediated amperometric biosensors (Willner, 1997; Scouten et al., 1995) but have received relatively little attention for protein film voltammetry (Jiang et al., 1995; Kuznetsov et al., 1994) despite the observation that submonolayers of cytochrome *c* carbodiimide coupled to carboxylate terminated alkane thiol:gold electrodes exhibit improved stability to variation of pH and ionic strength compared to protein adsorbed at the same surface (Collison et al., 1992). Here we report that Ifc_3 labeled with 2-pyridyl disulfide functionalities by reaction with N-succinimidyl 3-(2-pyridyldithio) propionate (SPDP; Carlsson et al., 1978) adsorbs on gold electrodes to give voltammetry indistinguishable from that of the native protein but with a stability to electrode rotation that permits further analysis of its fumarate reductase activity. This has allowed us to obtain evidence that when enzyme turnover occurs at rates exceeding half the maximum velocity the lowest potential heme plays a role in modulating the enzyme's rate of fumarate reduction.

MATERIALS AND METHODS

Ifc_3 was purified from *S. frigidimarina* NCIMB400 as described previously (Dobbin et al., 1999) and stored frozen in liquid nitrogen. Ifc_3 samples were prepared for study by diafiltration at 4°C in an Amicon 8MC unit (Millipore Corporation, Bedford, MA) equipped with microvolume assembly and YM3 membrane and typically showed an A_{410nm}/A_{280nm} ratio of 3.5. Protein concentrations were determined after dithionite reduction using $\epsilon_{552nm} = 110{,}000\ M^{-1} \cdot cm^{-1}$. Stock solutions of N-succinimidyl 3-(2-pyridyldithio)propionate, SPDP (Sigma-Aldrich Chemical Company Ltd., Poole, Dorset, UK) were prepared in >99.5% ethanol and concentrations determined with $\epsilon_{280nm} = 5100\ M^{-1} \cdot cm^{-1}$. All reactions and electrochemical experiments were performed in 100 mM NaH_2PO_4, 100 mM NaCl brought to pH 7.5 with NaOH unless otherwise stated, and this solution is referred to as buffer-electrolyte throughout. Sodium fumarate was added to the desired concentration from a 40 mM stock solution in buffer-electrolyte, pH 7.5. Reagents were of Analar quality or equivalent and all water was AnalaR (BDH Laboratory Supplies, Poole, Dorset, UK).

Reaction between SPDP and Ifc_3 was performed according to the method of Carlsson et al. (1978) with minor alterations. Aliquots of 20 mM SPDP stock solutions were added to a stirring, room temperature solution of 50 μM Ifc_3 to give a final concentration of 100 μM. After 30 min, separation of protein from low molecular weight species by gel filtration on a PD-10 column (Amersham Pharmacia Biotech, Uppsala, Sweden) was confirmed by UV-visible spectroscopy of the fractions (1 ml). The first two Ifc_3-containing fractions were pooled, concentrated by diafiltration, and used in subsequent experiments to characterize the SPDP-reacted Ifc_3. This sample will be referred to as 2-pyridyl disulfide-Ifc_3, which does not imply stoichiometric modification of the protein (see Results) but serves to distinguish it from the unlabeled Ifc_3 sample.

Release of pyridine 2-thione from 20 μM 2-pyridyl disulfide-Ifc_3 was performed by incubation with 400 μM dithiothreitol for 30 min in a stirring, room temperature solution. Separation of protein and pyridine 2-thione (λ_{max} 343 nm) was achieved either by gel filtration as described above or by diafiltration with a Microcon-30 microconcentrator (Millipore Corporation, Bedford, MA) and subsequent "washing" of the protein sample by two rounds of dilution and concentration after which no further pyridine 2-thione could be detected in the filtrate. Addition of further dithiothreitol to the reaction mixture or longer incubations of the reaction failed to liberate additional pyridine 2-thione. After pooling all appropriate fractions or filtrate, pyridine 2-thione was quantified using $\epsilon_{343\ nm} = 8080\ M^{-1} \cdot cm^{-1}$ (Carlsson et al., 1978).

Spectrophotometric determination of K_M for fumarate reduction by Ifc_3 in buffer-electrolyte was performed in stirred, anaerobic cuvettes using methyl viologen ($E_m = -445$ mV) as the electron donor, $\epsilon_{600nm} = 13{,}000\ M^{-1} \cdot cm^{-1}$ (Dobbin et al., 1999). After titration with sodium dithionite to give A_{600nm} of ~1, fumarate was added to concentrations of 0 to 100 μM and the reaction initiated with 1.3 nM Ifc_3. Assays to compare the fumarate reductase activity of Ifc_3 and 2-pyridyl disulfide-Ifc_3 were performed with 10 mM sodium fumarate. FPLC analysis was performed on a Mono-Q Anion Exchange column (Amersham Pharmacia Biotech, Uppsala, Sweden) equilibrated with 50 mM NaCl, 50 mM Tris-HCl, pH 8, and protein was eluted with a NaCl gradient in 50 mM Tris-HCl, pH 8. Surface enhanced laser desorption/ionization (SELDI) mass spectrometry (Ciphergen Biosystems Ltd., Camberley, UK) was with a Normal Phase Chip and EAM1 matrix.

Cyclic voltammetry was performed with an Autolab electrochemical analyzer (EcoChemie, Utrecht, The Netherlands) using the analog scan generator controlled by GPES software. The electrochemical cell, consisting of a platinum foil counter electrode and Ag/AgCl, KCl (saturated) reference electrode in a Luggin side arm, was thermostatted (25°C) and housed in an anaerobic chamber (Belle Technology, Portesham, UK) with O_2 content < 2 ppm. Electrode rotation was with an EG&G Model 636 Electrode Rotator (Princeton Applied Research, Princeton, NJ). Pyrolytic graphite "edge" (PGE) or gold working electrodes of geometric area 0.07 cm^2 were polished with an aqueous 0.3 μm Al_2O_3 slurry, sonicated, and rinsed thoroughly immediately before use. Electrodes exposed to 10 μM 2-pyridyl disulfide-Ifc_3 solutions were rinsed extensively with room temperature buffer-electrolyte before placing them in the electrochemical cell. SPDP-modified gold electrodes were prepared by overnight incubation in 10 μM SPDP, buffer-electrolyte, 4°C. All potentials are reported with reference to the standard hydrogen electrode (S.H.E.) by addition of 0.197 V to that measured at 25°C (Bard and Faulkner, 1980).

RESULTS

Characterization of 2-pyridyl disulfide-Ifc_3

After reaction of 100 μM SPDP with 50 μM Ifc_3 the extent of 2-pyridyl disulfide incorporation was found to be 1.3 $\pm$ 0.2 equivalents per Ifc_3 molecule based on release of pyridine 2-thione from three independently prepared samples. While nucleophilic attack on the N-hydroxysuccinimidyl-ester of SPDP may occur through protein primary amines or thiolates, reaction of Ifc_3 with SPDP is expected solely at lysine residues and/or the N-terminus, as illustrated in Fig. 1, since each of the protein's eight cysteine residues form thioether linkages to the *c*-hemes (Dobbin et al., 1999). FPLC anion exchange chromatography showed >95% of the 2-pyridyl disulfide-Ifc_3 sample to be derivatized eluting as a broad band (230 mM NaCl) compared to the sharp elution of Ifc_3 (200 mM NaCl). The molecular weight of 2-pyridyl disulfide-Ifc_3 determined by SELDI mass spectrometry was indistinguishable from that of Ifc_3 (M_r 63, 985 $\pm$ 0.5%) consistent with derivatization of the majority of protein molecules to the level of one or two 2-pyridyl disulfide functionalities.

UV-visible absorption spectra of air-oxidized 2-pyridyl disulfide-Ifc_3 and Ifc_3 were indistinguishable. Spectra of the reduced labeled protein were recorded immediately after dithionite addition to minimize any effects due to slow pyridine 2-thione release and showed no differences to spectra of dithionite-reduced Ifc_3 with peak maxima at 552 nm, 523 nm, and 420 nm (α-, β-, and γ-bands, respectively) (Dobbin et al., 1999). Functional integrity of 2-pyridyl disulfide-Ifc_3 was demonstrated in fumarate reductase assays that yielded turnover numbers of 320 $\pm$ 50 s^{-1} for both enzymes.

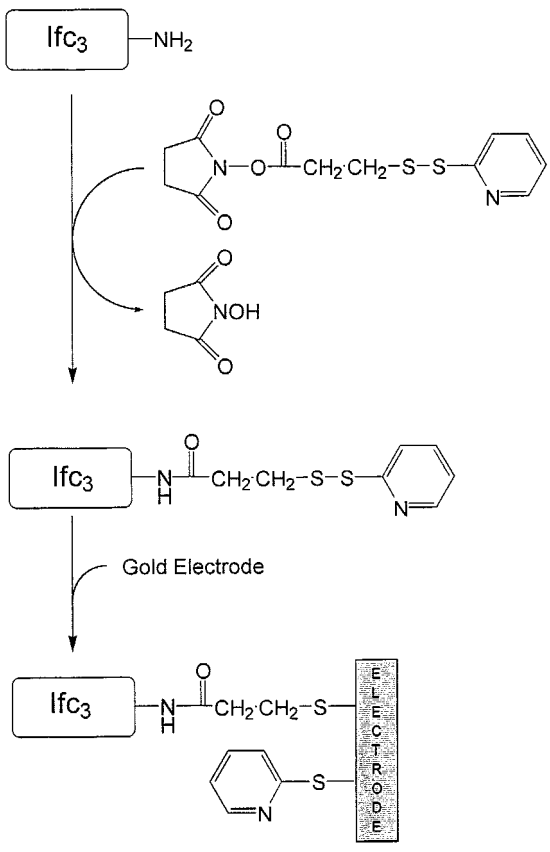

FIGURE 1 Proposed mechanism for the labeling of Ifc_3 with 2-pyridyl disulfide by SPDP and its subsequent immobilization as thiolated Ifc_3 on gold electrodes.

Electrochemistry of Ifc_3 adsorbed on gold and PGE electrodes

Gold electrodes placed in 0.5 μM Ifc_3 for 5 min at 25°C then rinsed with buffer-electrolyte to remove loosely bound protein show a clear catalytic reduction wave in 2 mM fumarate not observed before Ifc_3 adsorption (Fig. 2 *A*). Subsequent rinsing of the Ifc_3 gold electrode and transfer to a solution devoid of fumarate produces a voltammetric response indistinguishable from that obtained in the absence of Ifc_3, but on return to a 2 mM fumarate solution the catalytic reduction wave is restored to ~80% of its original magnitude (data not shown). The lack of noncatalytic waves prevents reduction potentials being determined for the immobilized enzyme's redox cofactors, but the position of the catalytic wave spanning from -150 to -400 mV is in good agreement with the redox properties of the enzyme determined in solution studies (Dobbin et al., 1999).

Cyclic voltammograms of Ifc_3 gold electrodes in 2 mM fumarate were independent of scan rate up to at least 20 mV $\cdot$ s^{-1} and after background subtraction the forward and reverse sweeps overlay one another, indicating that catalysis is occurring under steady-state conditions. Inspection of the catalytic wave shown in Fig. 2 *A* reveals the presence of overlapping features more clearly distinguished in the first derivative of catalytic current with respect to potential (d*i*/d*E*), Fig. 2 *B*. A prominent, symmetric feature centered on -173 $\pm$ 10 mV is accompanied by a smaller, broader component centered around -290 mV. PGE electrodes coated with Ifc_3 in a procedure identical to that described above produced almost indistinguishable catalytic waveforms to those seen at gold electrodes (Fig. 2 *B*), making it unlikely that the features on the catalytic waveform arise from an anomalous protein-electrode interaction.

Electrochemistry of thiolated Ifc_3 at gold electrodes

Analysis of Ifc_3 adsorbed on stationary gold or PGE electrodes at lower fumarate concentrations was complicated by the appearance of a peak in the catalytic response on sweeping to more negative potentials indicative of substrate depletion at the electrode surface (Bard and Faulkner, 1980).

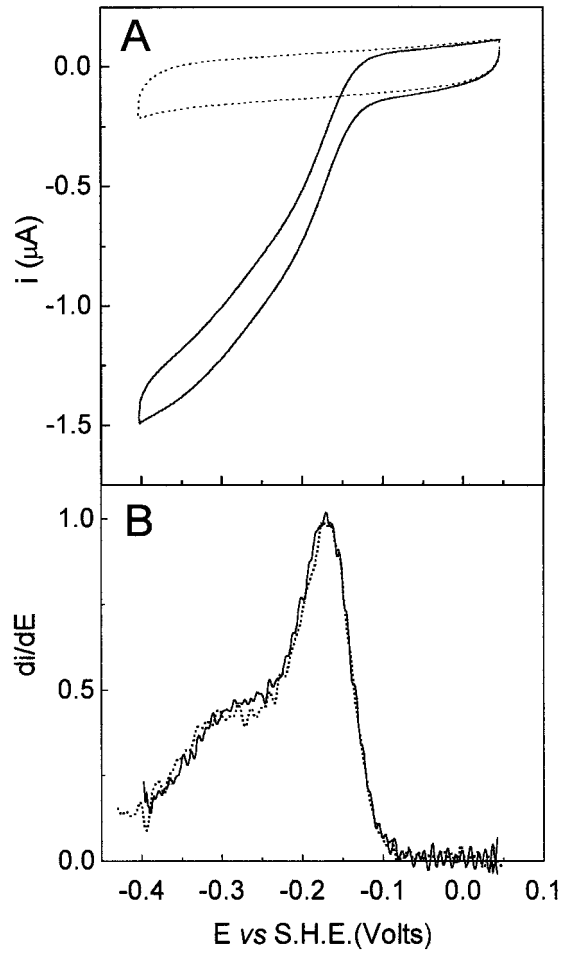

FIGURE 2 (*A*) Cyclic voltammograms of a gold electrode in 2 mM fumarate before (*dotted line*) and after (*solid line*) adsorption of Ifc_3. (*B*) Catalytic current derivatives with respect to applied potential of Ifc_3 adsorbed on gold (*dotted line*) and PGE (*solid line*) electrodes in 2 mM fumarate; the baseline-corrected derivative of the scan to increasingly negative potentials is shown normalized at −173 mV. Experimental conditions were scan rate 5 mV · s^{-1}, 100 mM NaH_2PO_4, 100 mM NaCl, pH 7.5, 25°C.

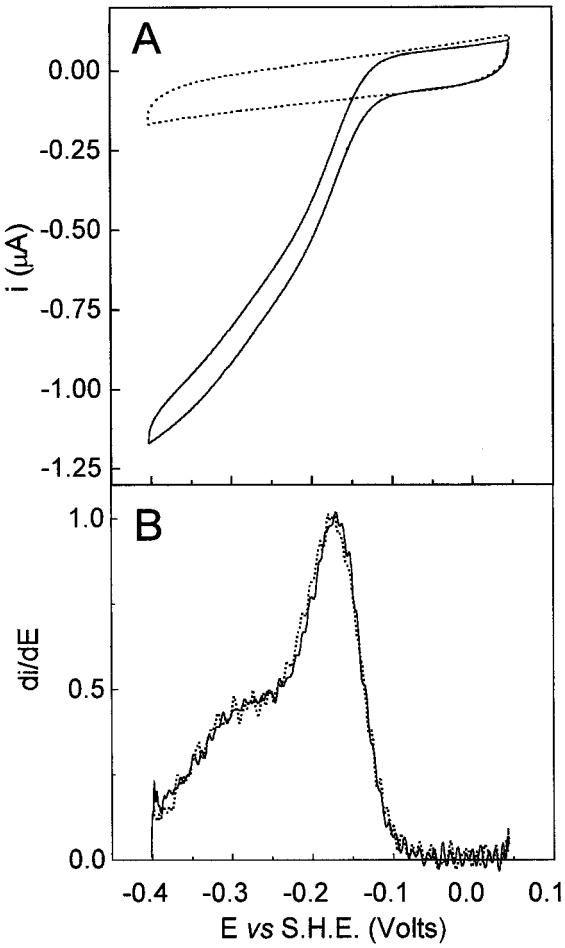

FIGURE 3 (*A*) Cyclic voltammograms of thiolated Ifc_3 chemisorbed on a gold electrode in 0 mM (*dotted line*) and 2 mM (*solid line*) fumarate, electrode rotation speed 2200 rpm. (*B*) Normalized catalytic current derivatives of thiolated Ifc_3 chemisorbed on gold with electrode rotation at 2200 rpm (*solid line*) and Ifc_3 adsorbed on gold at 0 rpm (*dotted line*). Experimental conditions as in Fig. 2.

Rotation of the electrodes was accompanied by a rapid decrease in signal amplitude, suggesting that protein was being spun off the electrode surface. By contrast, gold electrodes placed in 10 μM 2-pyridyl disulfide-Ifc_3 overnight at 4°C and rinsed thoroughly with buffer-electrolyte exhibited clear fumarate reductase activity, which was stable to electrode rotation (Fig. 3 *A*). The close similarity between the d*i*/d*E* plots of gold electrodes exposed to Ifc_3 or 2-pyridyl disulfide-Ifc_3 and placed in 2 mM fumarate (Fig. 3 *B*) demonstrates that the modification procedure results in negligible changes to the voltammetric response. Monolayer coverage of Ifc_3 is calculated to be $\sim 5 \times 10^{-12}$ mol · cm^{-2} from the unit cell dimensions of the crystallized protein (Bamford et al., 1999a). In the absence of substrate, the relationship between electroactive surface coverage, Γ^*, and the peak current, i_p, for immobilized redox molecules is

$$i_p = \frac{n^2F^2}{4RT}\upsilon A\Gamma^* \quad (1)$$

where n = number of electrons transferred, υ is the scan rate, A the electrode area, and R, T, and F have their usual meaning (Bard and Faulkner, 1980). Equation 1 predicts that a monolayer of Ifc_3 would give rise to clearly visible noncatalytic waves due to two-electron oxidation and reduction of the active site flavin; this is also the case when the apparent n value is greater than 1, as described below (Heering et al., 1997). Close examination of voltammetry recorded in the absence of fumarate (Fig. 3 *A*) provided no evidence for a noncatalytic response, indicating electroactive coverage is substantially submonolayer. In control experiments, electrodes incubated overnight in 10 μM Ifc_3, rinsed, and placed in 2 mM fumarate solutions showed no

evidence of catalytic activity, and SPDP-derivatized electrodes showed no evidence for Faradaic currents in the potential range of interest.

By comparison with the behavior of alkane disulfides on gold (Nuzzo et al., 1987), the enhanced stability of the response from gold electrodes exposed to 2-pyridyl disulfide-Ifc_3 most likely results from covalent coupling of the protein and electrode (Fig. 1). Thiolated Ifc_3 is immobilized, accompanied by 2-pyridyl sulfide (Ferretti, S., S. Paynter, D. J. Richardson, D. A. Russell, and K. E. Sapsford, submitted for publication) a molecule structurally similar to the promoters frequently used to derivatize gold electrodes for direct protein electrochemistry (Allen et al., 1984). As anticipated from the voltammetric behavior of Ifc_3 at "bare" gold electrodes, in this instance 2-pyridyl sulfide is not required to stabilize the protein film. Treating 2-pyridyl disulfide-Ifc_3 with dithiothreitol followed by removal of pyridine 2-thione by gel filtration results in thiol modified-Ifc_3, which forms electroactive films with comparable electrochemistry and stability to those prepared from 2-pyridyl disulfide-Ifc_3. Electrodes exposed to 2-pyridyl disulfide-Ifc_3 overnight and subsequently kept in buffer-electrolyte at room temperature lost ~60% of their activity in the first 6 h after preparation and a further 10% of activity was lost during the next 18 h. This loss of signal amplitude was not anticipated but may be a consequence of the dissociation of noncovalently bound FAD from the protein. Loss of the enzyme's FAD occurs during voltammetry of Ifc_3 solutions giving rise to a sharp wavepair (−261 mV, pH 7.5) from FAD adsorbed on the electrode surface. Aside from the loss of signal amplitude, the voltammetric response of the thiolated Ifc_3 gold electrodes showed no detectable changes over time. Thus, no additional electroactive species contributed to the responses recorded during these experiments.

The response of Ifc_3 to variation in fumarate concentration was determined by cyclic voltammetry with electrode rotation rates above 1800 rpm, where the catalytic current was found to be independent of rotation rate and the form of the voltammograms consistent with a steady-state catalytic response. After subtraction of voltammograms recorded in 0 mM fumarate, current magnitudes were calculated at −400 mV, where it was considered that the catalytic current had reached a limiting value. Extending the voltammograms to lower potentials resulted in the rapid onset of large reduction currents. This phenomenon, which was not related to the presence of Ifc_3, was enhanced on addition of fumarate and manifested itself in the failure of the di/dE plots to reach zero at the low potential extreme of the voltammetric sweep (Figs. 2, 3, and 5).

Fumarate titrations performed on electrodes prepared up to 6 h previously were corrected for loss of signal amplitude by measuring voltammograms in 2 mM fumarate at regular intervals, while titrations performed 10 or more hours after electrode preparation could be completed without significant signal loss. Comparable results were obtained by either method and a typical result is shown in Fig. 4. For an immobilized enzyme undergoing electrocatalysis unlimited by rates of interfacial electron transfer or substrate mass transport, the limiting catalytic current observed at the most negative potentials is determined by the intrinsic properties of the enzyme. Using the Michaelis-Menten description of enzyme kinetics to write an expression for the magnitude of the catalytic current analogous to the solution velocity description of enzyme kinetics gives

$$i_{cat} = \frac{i_{max} C_{fumarate}}{C_{fumarate} + K_M} \quad (2)$$

where i_{cat} is the catalytic current magnitude at a given fumarate concentration, $C_{fumarate}$, K_M is the Michaelis constant of adsorbed enzyme, and i_{max} the current magnitude when $C_{fumarate}$ greatly exceeds K_M. If interfacial electron transfer rates are lower than the turnover number of enzyme, i_{cat} will reflect the slower process and the observed K_M will lie below the true K_M. The experimental data fit well to Eq. 2, yielding $K_M = 56 \pm 20$ μM, in good agreement with the value of 36 ± 20 μM determined in solution assays using methyl viologen as the electron donor. Thus, the activity of the immobilized enzyme is comparable to that of the protein in solution. Moreover, the assumption is validated that at most negative potentials enzyme turnover is not limited by rates of interfacial electron exchange.

As illustrated by the catalytic current derivative in Fig. 5 (*dotted line*) the voltammetric response in 55 μM fumarate is composed of one feature centered at $E_{max} = -205$ mV. On increasing the fumarate concentration two major changes occur. The catalytic wave becomes displaced to increasingly positive potentials, Fig. 5, *inset*, and at fumarate concentrations above 145 μM a second, broader feature

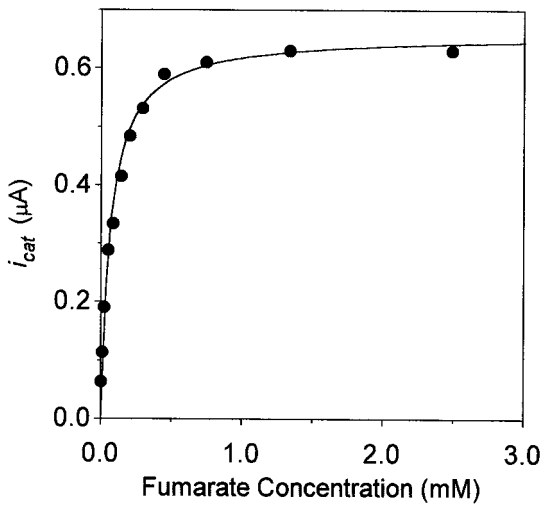

FIGURE 4 Variation of the catalytic current magnitude with fumarate concentration for thiolated Ifc_3 chemisorbed on a gold electrode, rotation rate 2200 rpm. The solid line shows a fit to the Michaelis-Menten description of enzyme kinetics with $K_M = 55$ μM and $i_{max} = 0.659$ μA.

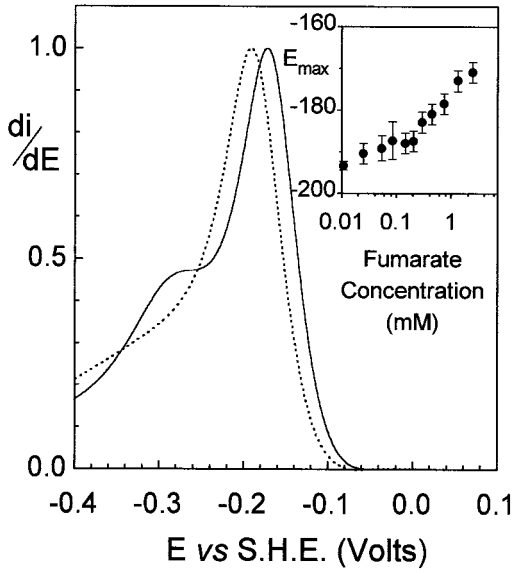

FIGURE 5 Catalytic current derivatives of thiolated Ifc_3 chemisorbed on a gold electrode in 55 μM (*dotted line*) and 2.49 mM (*solid line*) fumarate. To compensate for the relatively high signal-to-noise in the voltammogram recorded at 55 μM fumarate, voltammograms for both fumarate concentrations have been smoothed by fast Fourier transform. *Inset:* The influence of fumarate concentration on the position of the high potential maximum, E_{max} (mV), in the catalytic current derivative. Electrode rotation rate 2000 rpm; all other conditions as in Fig. 2.

centered around −290 mV becomes increasingly apparent (Fig. 5, *solid line*). At 2 mM fumarate the low potential component of the catalytic wave contributes ~35% of i_{cat}, as illustrated in Figs. 2 and 3. The steepness of the catalytic wave in cyclic voltammograms contains information on the number of electrons transferred in the rate-determining event in catalysis (Heering et al., 1997, 1998; Bard and Faulkner, 1980). This information is readily extracted from the half-height width, $\delta_{1/2}$, of the catalytic current derivative since

$$\delta_{1/2} = 3.53\ RT/n_{app}F \qquad (3)$$

Integer values will be obtained for the apparent n value, n_{app}, in the case of ideal electron transfer reactions, while non-integer values will reflect the presence of nonidealities such as coupled reactions.

Examination of the catalytic current derivative of Ifc_3 at fumarate concentrations below 145 μM reveals that where both flanks of the wave can be clearly resolved they are symmetrical. Superposition of normalized, theoretical waveshapes for the catalytic current derivatives of $n = 1$ and $n = 2$ processes (Heering et al., 1997) on the experimental results showed that for Ifc_3, $1 < n_{app} < 2$. Quantitative analysis was performed on the high-potential flank of the derivative to minimize broadening introduced by failure of the derivative to reach zero toward more negative potentials. The half-height width of the high-potential flank was doubled to give $\delta_{1/2}$ yielding a value of $n_{app} = 1.25$ (the maximum deviation from the average of over 20 determinations was ±0.1). No broadening of this component of the catalytic wave could be detected over the entire range of fumarate concentrations investigated. The lower potential component of the catalytic response was analyzed in derivatives obtained at fumarate concentrations of 2 mM or above where this feature was most pronounced. For simplicity it was considered that the derivative consisted of two components whose sum produced the observed response. Addition of an $n_{app} = 1$ wave centered on −290 mV to that of the $n_{app} = 1.25$ wave (in ratio 0.4:1 at 2 mM fumarate) reproduced well the main features of the derivative. It was noted that this procedure always underestimated the magnitude of the derivative below −300 mV and between −200 and −240 mV, but due to the uncertain nature of the background contributions a more stringent fitting of the data was considered unwarranted.

An interesting comparison can be made between the observations made with Ifc_3 and the predictions of Heering et al. for the shape and position of the catalytic waveform arising from an immobilized enzyme array undergoing steady-state catalysis under various limiting conditions (Heering et al., 1998). Displacement of the major, high-potential component of the catalytic wave to increasingly positive potentials with increasing substrate concentration is consistent with neither mass transport nor interfacial electron transfer being rate-limiting steps. Rather, intrinsic enzyme kinetics determine the form of the voltammogram whether electron exchange with the electrode is direct to the catalytic site or via an intermediate redox cofactor (heme in this case) followed by rapid intramolecular electron transfer to the catalytic site. In either case the width of the wave yields an apparent n value greater than one reflecting cooperativity of addition of the two electrons required to reduce the catalytic FAD site. However, at fumarate concentrations 10-fold above K_M the displacement of the catalytic response is less than the limiting magnitude for an $n = 2$ process, $+59/n$ mV per log $C_{fumarate}$ at 25°C (Heering et al., 1998). This suggests the interesting possibility that at high fumarate concentrations the rate of electron delivery to FAD by the high-potential pathway becomes slow relative to the rate of substrate turnover at the active site. To compensate for this, electron delivery to the active site is boosted below −240 mV, producing the second feature in the voltammetric response and ensuring that the full catalytic potential of the enzyme is realized. Since the lower potential, $n \approx 1$, component of the catalytic wave is centered around −290 mV, this implicates the lowest potential heme of Ifc_3, $E_m = -259$ mV (Dobbin et al., 1999), as having a defining role in the rate of fumarate reduction under conditions of high turnover rates at pH 7.5.

DISCUSSION

Bifunctional reagents such as SPDP represent a convenient method with which to introduce immobilization sites onto protein surfaces. They permit rapid assessment of the feasibility of immobilizing proteins as electroactive arrays before performing more site-specific methods for introducing immobilization loci, such as by genetic engineering (Wood et al., 1997; Firestone et al., 1996; Vigmond et al., 1994). A wide variety of bifunctional reagents are available for introducing thiol/disulfide labels onto proteins (King et al., 1978; Wilchek and Miron, 1972; Perham and Thomas, 1971) and for proteins exhibiting direct electron exchange with gold or modified gold electrodes, these present a general method for stabilizing the protein-electrode interface by covalent gold-sulfur linkage.

SPDP protein labeling is most likely to occur in a random manner. Thus, despite the presence of one or two 2-pyridyl disulfide moieties per Ifc_3, the adsorbed array used in these studies is anticipated to contain a range of protein orientations of which only some are suitable for direct electron exchange with the electrode. Indeed, 2-pyridyl disulfide-Ifc_3 was consistently found to immobilize as a submonolayer of electroactive material, and while this prevented direct determination of the reduction potentials of the immobilized protein there were no other discernible disadvantages of random derivatization. It is unlikely that the features observed in the electrocatalytic response at high fumarate concentrations arise from distinct populations of immobilized enzyme, since their relative magnitude was identical at PGE and gold electrodes, materials which present very different surfaces for protein adsorption.

Information on the mechanism of fumarate reduction by Ifc_3 is contained in the voltammetric waveform whose complexity reflects modulation of the enzyme's catalytic activity in response to applied potential. Of particular note is the presence of two features in the catalytic wave obtained at fumarate concentrations greater than $2 \times K_M$. Voltammetry of another multicentered fumarate reductase, FrdAB of *E. coli,* shows similar behavior to that reported here and has been proposed to arise from the operation of parallel intramolecular electron transfer pathways (Heering et al., 1997). Iron-sulfur centers 1 and 3 with reduction potentials around -50 mV relay electrons to the active site via a low driving force route compared to relay via iron-sulfur center 2 with a reduction potential ~ -300 mV. By possessing multiple or bifurcated electron transfer pathways, enzymes that perform cooperative $n \geq 2$ electron transformations are provided a means with which to couple electron transfer to their $n = 1$ redox cofactors and the arrangement of hemes in *Nitrosomonas europaea* hydroxylamine oxidoreductase (Igarashi et al., 1997) supports the validity of this strategy. Two multiheme pathways leave the active site and are proposed to partition the four electrons released in hydroxylamine oxidation to two distinct outlet sites, for utilization by either cytochrome *c* oxidase or ammonia monooxygenase.

The high potential pathway for electron delivery to the active site of Ifc_3 shows cooperative two-electron reduction of FAD consistent with the results from EPR monitored potentiometric titrations, which provided no evidence for the existence of a stable flavin semiquinone (Dobbin et al., 1999). Whether this pathway consists only of protein matrix or includes the heme centers has not been resolved by this work. However, at fumarate concentrations twofold greater than K_M reduction of the lowest potential heme clearly boosts the rate of fumarate reduction. It is unlikely that modulation of the lowest potential heme's oxidation state influences fumarate reduction through a change in the level of protonation of the protein, since this would lead to a two-component wave at all fumarate concentrations. Communication between the cofactors of Ifc_3 could lead to the redox state of the lowest potential heme regulating electron flux through the high potential pathway. However, by analogy with *E. coli* FrdAB (Heering et al., 1997) and hydroxylamine oxidoreductase (Igarashi et al., 1997), we favor an alternative interpretation in which the lowest potential heme relays electrons to the catalytic site by a pathway distinct from that already being utilized with a lower driving force at more positive potentials (Fig. 6). Whether the dual electron transfer pathways operate in parallel or converge to form a bifurcated system funneling electrons to the active site, their combination ensures that electron delivery to the active site is always rapid relative to the active site's rate of

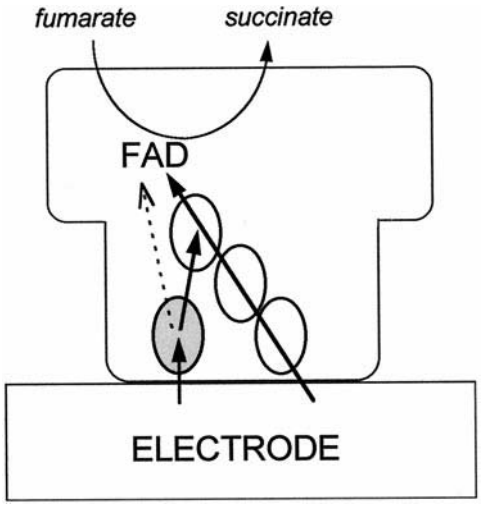

FIGURE 6 Schematic illustration of the dual electron transfer pathways (proposed to operate) during fumarate reduction by Ifc_3 immobilized on an electrode surface. The lowest potential heme (*shaded*) is shown acting as a one-electron relay and the involvement of all four hemes in electron delivery to the active site is implied; see text. In a bifurcated pathway (*solid lines*) the lowest potential heme must lie upstream of the convergence point. The broken line indicates a route for electron transfer from the lowest potential heme to the active site by a pathway parallel to that operating at lower driving force.

substrate transformation. In vivo, Ifc_3 most probably receives electrons derived from the cytoplasmic membrane entrapped quinol pool via the membrane-anchored cytochrome CymA (Dobbin et al., 1999; Field, S. J., P. S. Dobbin, M. R. Cheesman, A. J. Thomson, and D. J. Richardson, submitted for publication). This protein contains hemes with reduction potentials of +10, −108, −136, and −229 mV (pH 7.5) suggesting that the lowest potential heme of Ifc_3 could be reduced under physiological conditions.

By resolving enzyme activity in the potential domain, direct electrochemistry of Ifc_3 has provided kinetic evidence for the operation of dual electron transfer pathways through the protein. Whether these pathways operate in parallel or converge to form a bifurcated system cannot be resolved from the voltammetric data alone. However, together with the recently available structure of Ifc_3 (Bamford et al., 1999b) which shows two heme "arms" converging to the active site, it is proposed that a bifurcated electron transfer pathway operates within Ifc_3.

The authors thank Drs. David Russell and Silvia Ferretti for suggesting the use of SPDP, A. Cavill of the Sainsbury Laboratory, John Innes Centre, Norwich for access to and assistance with SELDI mass spectrometry facilities, and Dr. Myles Cheesman for helpful discussions.

J. N. B. gratefully acknowledges the Wellcome Trust for a Research Career Development Fellowship, Grant 050709.

D. J. R. and P. S. D. also thank the Wellcome Trust for funding by project grant 046547.

REFERENCES

Allen, P. M., H. A. O. Hill, and N. J. Walton. 1984. Surface modifiers for the promotion of direct electrochemistry of cytochrome c. *J. Electroanal. Chem.* 178:69–86.

Armstrong, F. A. 1990. Probing metalloproteins by voltammetry. *Struct. Bond.* 72:137–221.

Armstrong, F. A., H. A. Heering, and J. Hirst. 1997. Reactions of complex metalloproteins studied by protein-film voltammetry. *Chem. Soc. Rev.* 26:169–179.

Bamford, V., P. S. Dobbin, S-C. Lee, A. Reilly, A. K Powell, D. J. Richardson, and A. M. Hemmings. 1999a. Crystallization and preliminary x-ray crystallographic analysis of a periplasmic tetrahaem flavocytochrome c_3 from *Shewanella frigidimarina* NCIMB400. *Acta. Crystallogr. D.* 50:1222–1225.

Bamford, V., P. S. Dobbin, D. J. Richardson, and A. M. Hemmings. 1999b. Open conformation of a flavocytochrome c_3 fumarate reductase. *Nat. Struct. Biol.* 6:1104–1107.

Bard, A. J., and L. R. Faulkner. 1980. Electrochemical Methods. Fundamentals and Applications. John Wiley and Sons, Inc. New York.

Butt, J. N., A. Sucheta, F. A. Armstrong, J. Breton, A. J. Thomson, and E. C. Hatchikian. 1993. Voltammetric characterization of rapid and reversible binding of an exogenous thiolate ligand at a [4Fe-4S] cluster in Ferredoxin III from *Desulfovibrio africanus. J. Am. Chem. Soc.* 115:1413–1421.

Carlsson, J., H. Drevin, and R. Axén. 1978. Protein thiolation and reversible protein-protein conjugation. *Biochem. J.* 173:723–737.

Chapman, S. K., F. Welsh, R. Moysey, C. Mowat, M. K. Doherty, K. L. Turner, A. W. Munro, and G. A. Reid. 1999. Flavocytochromes: transceivers and relays in biological electron transfer. *Biochem. Soc. Trans.* 27:185–189.

Chidsey, C. E. D. 1991. Free energy and temperature dependence of electron transfer at the metal-electrolyte interface. *Science.* 251: 919–922.

Collison, M., E. F. Bowden, and M. J. Tarlov. 1992. Voltammetry of covalently immobilized cytochrome c on self-assembled monolayer electrodes. *Langmuir.* 8:1247–1250.

Daff, S., W. J. Ingledew, G. A. Reid, and S. K. Chapman. 1996. New insights into the catalytic cycle of flavocytochrome b_2. *Biochemistry*. 35:6345–6350.

Dobbin, P. S., J. N. Butt, A. K. Powell, G. A. Reid, and D. J. Richardson. 1999. Characterization of a flavocytochrome that is induced during the anaerobic respiration of Fe^{3+} by *Shewanella frigidimarina* NCIMB400. *Biochem. J.* 342:439–448.

Firestone, M. A., M. L. Shank, S. G. Sligar, and P. W. Bohn. 1996. Film architecture in biomolecular assemblies. Effect of linker of the orientation of genetically engineered surface-bound proteins. *J. Am. Chem. Soc.* 118:9033–9041.

Heering, H. A., J. Hirst, and F. A. Armstrong. 1998. Interpreting the catalytic voltammetry of electroactive enzymes adsorbed on electrodes. *J. Phys. Chem. B.* 102:6889–6902.

Heering, H. A., J. H. Weiner, and F. A. Armstrong. 1997. Direct detection and measurement of electron relays in a multicentered enzyme: voltammetry of electrode-surface films of *E. coli* fumarate reductase, an iron-sulfur flavoprotein. *J. Am. Chem. Soc.* 48:11628–11638.

Hirst, J., J. L. C. Duff, G. N. L. Jameson, M. A. Kemper, B. K. Burgess, and F. A. Armstrong. 1998a. Kinetics and mechanism of redox-coupled, long-range proton transfer in an iron-sulfur protein. Investigation by fast-scan protein-film voltammetry. *J. Am. Chem. Soc.* 120:7085–7094.

Hirst, J., G. N. L. Jameson, J. W. A. Allen, and F. A. Armstrong. 1998b. Very rapid cooperative two electron/two proton redox reactions of [3Fe-4S] Clusters: detection and analysis by protein film voltammetry *J. Am. Chem. Soc.* 120:11994–11999.

Hirst, J., A. Sucheta, B. A. C. Ackrell, and F. A. Armstrong. 1996. Electrocatalytic voltammetry of succinate dehydrogenase: direct quantification of the catalytic properties of a complex electron-transport enzyme. *J. Am. Chem. Soc.* 118:5031–5038.

Igarashi, N., H. Moriyama, T. Fujiwara, Y. Fukomori, and N. Tanaka. 1997. The 2.8 Å structure of the hydroxylamine oxidoreductase from a nitrifying chemoautotrophic bacterium, *Nitrosomonas europaea. Nat. Struct. Biol.* 4:276–284.

Jiang, L., C. J. McNeil, and J. M. Cooper. 1995. Direct electron transfer reactions of glucose oxidase immobilized at a self-assembled monolayer. *J. Chem. Soc. Chem. Commun.* 1293–1295.

King, T. P., Y. Li, and L. Kochoumian. 1978. Preparation of protein conjugates via intermolecular disulfide bond formation. *Biochemistry.* 17:1499–1506.

Kuznetsov, B. A., N. A. Byzova, and G. P. Shumakovich. 1994. The effect of orientation of cytochrome c molecules covalently attached to the electrode surface upon their electrochemical activity. *J. Electroanal. Chem.* 371:85–92.

Nuzzo, R. G., B. R. Zegarski, and L. H. Dubois. 1987. Fundamental studies of the chemisorption of organosulfur compounds on Au(111). Implications for molecular self-assembly on gold surfaces. *J. Am. Chem. Soc.* 109:733–740.

Perham, N. R., and J. O. Thomas. 1971. Reaction of tobacco mosaic virus with a thiol-containing imodoester and a possible application to x-ray diffraction analysis. *J. Mol. Biol.* 62:415–418.

Saraste, M. 1999. Oxidative phosphorylation at the fin de siècle. *Science.* 283:1488–1493.

Scouten, W. H., J. H. T. Luong, and R. S. Brown. 1995. Enzyme or protein immobilization methods for applications in biosensor design. *TIBTECH* .13:178–185.

Turner, K. L., M. K. Doherty, H. A. Heering, F. A. Armstrong, G. A. Reid, and S. K. Chapman. 1999. Redox properties of flavocytochrome c_3 from *Shewanella frigidimarina* NCIMB400. *Biochemistry.* 38:3302–3309.

Vigmond, S. J., M. Iwakura, F. Mizutani, and T. Katsura. 1994. Site-

specific immobilization of molecularly engineered dihydrofolate reductase to gold surfaces. *Langmuir.* 10:2860–2862.

Weber, K., and S. E. Creager. 1994. Voltammetry of redox-active groups irreversibly adsorbed onto electrodes. Treatment using the Marcus relation between rate and overpotential. *Anal. Chem.* 66:3164–3172.

Wightman, R. M. 1981. Microvoltammetric electrodes. *Anal. Chem.* 53: 1125A—1134A.

Wilchek, M., and T. Miron. 1972. The conversion of tryptophan to 2-thioltryptophan in peptides and proteins. *Biochem. Biophys. Res. Commun.* 47:1015–1020.

Willner, I. 1997. Photoswitchable biomaterials: en route to optobioelectronic systems. *Acc. Chem. Res.* 30:347–356.

Wood, L. L., S-S. Cheng, P. L. Edmiston, and S. S. Saavedra. 1997. Molecular orientation distributions in protein films. 2. Site-directed immobilization of yeast cytochrome *c* on thiol capped self-assembled monolayers. *J. Am. Chem. Soc.* 119:571–576.